

## A Group Theoretical Paradigm for describing the Skeletal Molecular Orbitals of Cluster Compounds. Part 1. Deltahedral Clusters

Roy L. Johnston and D. Michael P. Mingos\*

*Inorganic Chemistry Laboratory, University of Oxford, South Parks Road, Oxford OX1 3QR*

Group theory and the Pairing Principle, inherent in Stone's Tensor Surface Harmonic Theory, have been applied to deltahedral clusters. Four classes of deltahedral cluster have been identified on the basis of their topological characteristics. Each of the classes has a characteristic spectrum of frontier molecular orbitals which determines the nature of deviations from the  $(N + 1)$  skeletal electron pair rule.

A central feature of the Polyhedral Skeletal Electron Pair Approach is the  $(N + 1)$  electron pair rule for  $N$ -vertex *closo* deltahedra and their *nido*- and *arachno*-derivatives.<sup>1</sup> Stone<sup>2</sup> has developed an elegant and general theoretical justification of this rule, based on the assumption that the deltahedral clusters are pseudo-spherical. Stone's Tensor Surface Harmonic Theory constructs a set of approximate molecular orbitals from the solution of the Schrödinger equation for a particle on a sphere. As in other situations where the free electron model works well, *e.g.* conjugated polyenes, the ordering of energy levels is determined by the nodal characteristics of the orbitals rather than their detailed forms. Therefore, even within a semi-empirical framework such calculations generally predict the correct ordering of molecular orbitals and the closed shell requirements.<sup>3</sup>

It is apparent, however, that for many deltahedra the  $(N + 1)$  rule is not always strictly adhered to and a significant number of departures from the rule occur. Fowler<sup>4</sup> has suggested that for  $N = 4$  the tetrahedron represents an 'intrinsic' exception to the  $(N + 1)$  rule, whereas the halogenoboranes  $B_8Cl_8$  and  $B_9Cl_9$  represent 'accidental' departures which result from the occurrence of several non-degenerate molecular orbitals in the frontier orbital region. Wade and O'Neill<sup>5</sup> have listed the symmetries of the frontier orbitals of the deltahedral borane clusters  $[B_nH_n]^{2-}$  and noted that some of the departures from the electron counting rules arise from the presence of non-degenerate highest occupied molecular orbitals (h.o.m.o.s). It is the purpose of our work to provide a fundamental derivation of the frontier orbital properties of deltahedral clusters and thus to explain how and why deviations from the  $(N + 1)$  rule occur. In this paper we demonstrate, for the first time, that there are four classes of convex deltahedral clusters with alternative and distinctive patterns of departure from the  $(N + 1)$  rule. These classes have been identified using group theoretical arguments in conjunction with the Pairing Principle inherent in Stone's Tensor Surface Harmonic analysis. The group theoretical bases of these arguments have previously been discussed by Fowler,<sup>4</sup> Ceulemans,<sup>6</sup> and Quinn and co-workers.<sup>7</sup>

### Results and Discussion

*Four Classes of Deltahedra.*—The nomenclature and definitions of the four classes of deltahedral clusters is presented here along with a hierarchical method for determining to which class a particular cluster belongs. Sub-classes are also indicated where appropriate. Later sections deal with each of the classes and sub-classes in detail.

If a deltahedral cluster is centrosymmetric and all of its atoms are identical and lie on the surface of the same sphere then the cluster belongs to class 1 (centrosymmetric spherical

deltahedra). If not then the principal rotation axis ( $C_n$ ) must be considered. If only one atom lies on the principal axis the cluster belongs to class 2 (polar deltahedra). Subdivision of this class depends on whether the principal axis is  $C_3$  [2(i)],  $C_2$  [2(ii)], or  $C_1$  [2(iii)]. The last case obviously corresponds to no rotational symmetry at all. When there are two atoms on the principal axis the cluster belongs to class 3 (bipolar deltahedra). Class 3 may be subdivided into 3(i) [bipyramidal ( $D_{nh}$ )] and 3(ii) [bicapped antiprismatic ( $D_{nd}$ )]. By continuing to stack layers further  $D_{nh}$  and  $D_{nd}$  deltahedra arise but these are significantly non-spherical fused polyhedra and, as such, are beyond the scope of this work. Finally if there are no atoms on the principal axis then the cluster belongs to class 4 (non-polar deltahedra). This class can be subdivided according to whether the atoms around the middle of the cluster lie on the equatorial plane [4(i),  $D_{3h}$ , planar equatorial] or form a puckered ring around the equator [4(ii),  $D_{nd}$ , puckered equatorial].

*Class 1: Centrosymmetric Spherical Deltahedra.*—The octahedron ( $O_h$ ) and icosahedron ( $I_h$ ) most closely approximate to spherical and consequently Stone's Tensor Surface Harmonic Theory gives the coefficients of the radial ( $L^\sigma$ ) and tangential ( $L^\pi, \bar{L}^\pi$ ) molecular orbitals precisely. The centrosymmetric nature of these polyhedra ensures that the odd-parity ( $\bar{L}^\pi$ ) orbitals cannot mix with their even-parity ( $L^\pi$ ) counterparts, because they have opposite symmetry with respect to the inversion operation ( $i$ ). The  $L^\pi$  and  $\bar{L}^\pi$  functions are related by the parity inversion operator ( $\hat{\epsilon}$ ) which transforms as  $\Gamma_u^0$  (*i.e.* anti-symmetric with respect to all improper rotations, reflections, and inversion) and which interconverts their bonding and antibonding character as shown below ( $\oplus$  is tensor addition,  $\otimes$  is tensor multiplication,  $n = \text{integer}$ ).

$$\begin{array}{ccc}
 L^\pi & & \Gamma_\pi = \Gamma_g^L (L = 2n) \oplus \Gamma_u^L (L = 2n + 1) \\
 \hat{\epsilon} \downarrow & & \downarrow \otimes \Gamma_u^0 \\
 \bar{L}^\pi & & \Gamma_{\bar{\pi}} = \Gamma_u^{\bar{L}} (\bar{L} = 2n) \oplus \Gamma_g^{\bar{L}} (\bar{L} = 2n + 1)
 \end{array}$$

Thus the high symmetry of these molecules ensures that the  $L^\pi$  and  $\bar{L}^\pi$  orbitals are symmetrically disposed about the non-bonding energy line (see Figure 1 for example). The parity inversion operator in these cases ensures the absence of self-conjugate non-bonding ( $L^\pi/\bar{L}^\pi$ )  $E$  pairs. Consequently the  $(N + 1)$  rule is rigorously applicable in such situations. Examples of such clusters include  $[B_6H_6]^{2-}$  (octahedral) and  $[B_{12}H_{12}]^{2-}$  (icosahedral). Departures from the  $(N + 1)$  rule will only occur

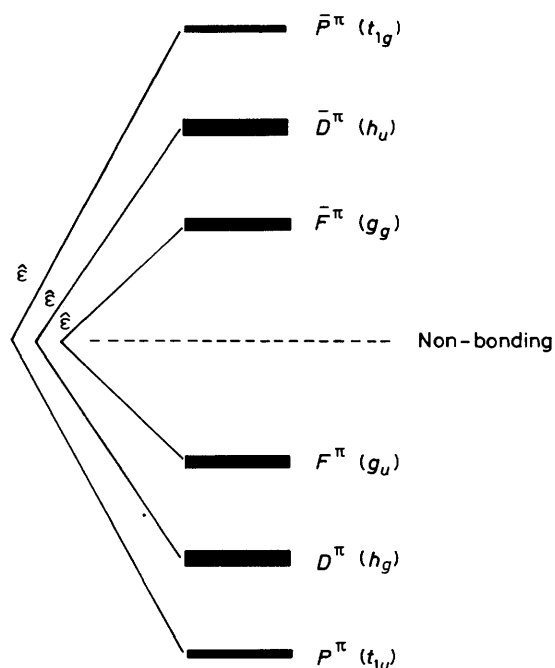
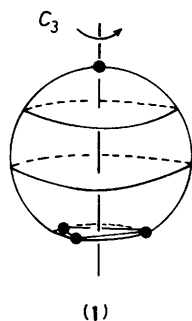


**Figure 1.** The  $L^*$  and  $\bar{L}^*$  orbitals of an icosahedral cluster, as an example of a centrosymmetric spherical cluster. The interconversion of  $L^*$  and  $\bar{L}^*$  by the parity inversion operator ( $\hat{\epsilon}$ ) is shown along with the resulting mirror image relationship of these orbitals about the non-bonding level



in situations where the clusters are significantly distorted from the idealised geometries.

**Class 2: Polar Deltahedra.**—Polar deltahedra are defined such that they possess one cluster vertex on each principal rotation axis. Three sub-classes may be distinguished, depending on the nature of these rotation axes.

(i)  $C_3$  *Polar deltahedra*. In this sub-class of polar deltahedra the axis on which the polar atom lies (polar axis) also passes perpendicularly through the centroid of a triangular face of the cluster (1) making it a  $C_3$  axis. Such clusters belong to the point groups  $C_3$ ,  $C_{3v}$ ,  $T$ , or  $T_d$  and possess one cluster atom on each principal ( $C_3$ ) rotation axis.<sup>8</sup> In a  $C_3$  or  $C_{3v}$  deltahedron there are  $P$  sets (layers) of symmetry related atoms lying in planes perpendicular to the  $C_3$  axis, consequently the total number of atoms in polar deltahedra must be  $(3P + 1)$ . The higher symmetry  $T$  or  $T_d$  possibilities arise from the occurrence of three additional three-fold symmetry axes, but only those polyhedra with  $(3P + 1)$  atoms have a single atom on each of these axes and may be classified as polar deltahedra.

For each of the  $P$  triangles of symmetry related atoms, the  $L^\sigma$  orbitals gives rise to  $A_1$  and  $E$  irreducible representations. The  $L^\sigma$  orbitals of a cluster belonging to an axial point group can be

obtained by combining the  $L^\sigma$  orbitals of its constituent orbits (*i.e.* sets of symmetry related atoms). Quinn and co-workers<sup>7</sup> have shown that the  $\pi\theta$  components of  $L^*$  and  $\bar{L}^*$  can be derived by using the  $L^\sigma$  orbitals as generator functions with a basis set of  $p_\theta^\pi$  orbitals (with the same local symmetry properties as  $p_z$  orbitals) rather than radial orbitals. In group theoretical terms this corresponds to the direct product (1).

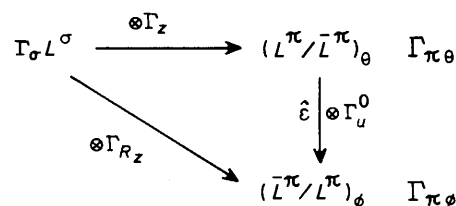
$$\Gamma_{\pi\theta} = \Gamma_\sigma \otimes \Gamma_z \quad (1)$$

The  $\pi\phi$  components are generated by taking the  $\pi\theta$  components and rotating the  $p^\pi$  orbital on each atom by  $90^\circ$  (in the same sense) about a radial vector. This process corresponds to the action of the parity inversion operator ( $\hat{\epsilon}$ ). In axial point groups the symmetry of the parity inversion operator is given by the direct product (2). Thus the  $\pi\phi$  component is obtained from  $L^\sigma$  orbitals by taking the direct product (3) ( $R_z$  represents

$$\Gamma_u^0 = \Gamma_z \otimes \Gamma_{R_z} \quad (2)$$

$$\Gamma_{\pi\phi} = \{\Gamma_\sigma \otimes \Gamma_z\} \otimes \{\Gamma_z \otimes \Gamma_{R_z}\} = \Gamma_\sigma \otimes \Gamma_{R_z} \quad (3)$$

rotation about the  $z$  axis). This information is summarised below.



In the  $C_{3v}$  point group, for example,  $\Gamma_z = A_1$  and  $\Gamma_{R_z} = A_2$ . Since  $E \otimes A_1$  or  $E \otimes A_2 = E$  then for every  $E$  function in  $L^\sigma$  there will be one in  $(L^\pi/\bar{L}^\pi)_\theta$  and one in  $(L^\pi/\bar{L}^\pi)_\phi$ . The total number of  $E$  representations in the  $L^\pi/\bar{L}^\pi$  orbitals is therefore even ( $2P$ ). When considering polyhedra with vertices lying on the  $C_3$  axis the above method for generating  $L^\pi/\bar{L}^\pi$  orbitals does not work because at the poles of a sphere an atomic  $p_z$  orbital has pure radial rather than tangential orientation (at any other position it can be resolved into radial and tangential components). To overcome this problem it is merely necessary to work out the orbitals for the non-polar structure and add the orbitals of the polar atoms. For one polar atom in  $C_{3v}$  symmetry the  $p^\pi$  atomic orbitals ( $p_x$  and  $p_y$ ) transform as  $E$  so the polar deltahedron possesses in total an odd number ( $2P + 1$ ) of  $E$  representations in the  $L^\pi/\bar{L}^\pi$  orbitals. This results in an equal number ( $P$ ) of bonding ( $L^\pi$ ) and antibonding ( $\bar{L}^\pi$ )  $E$  functions and one self-conjugate ( $L^\pi/\bar{L}^\pi$ )  $E$  set which is roughly non-bonding. These orbitals are singly noded with respect to the polar axis and as such are denoted  $(L^\pi/\bar{L}^\pi)_{\pm 1}$  [for example  $(D^\pi/\bar{D}^\pi)_{\pm 1}$  in the case of the tetrahedron ( $P = 1$ ) and  $(F^\pi/\bar{F}^\pi)_{\pm 1}$  in the case of the ten-vertex cluster ( $P = 3$ )]. In cases other than the tetrahedron (where all the vertices are equivalent by symmetry) the frontier pair of orbitals are predominantly localised on the polar atom. Occupation of these orbitals would lead to a cluster with  $(N + 2)$  skeletal electron pairs but usually they are unoccupied and an  $N$  skeletal electron pair count is observed.

Examples of polar deltahedral clusters possessing  $C_3$  axes and  $N$  or  $(N + 2)$  skeletal electron pairs are depicted in Figure 2. This class of cluster includes capped-deltahedra as well as the (ten-vertex)  $C_{3v}$  *hypercloso* clusters discussed by Greenwood and co-workers,<sup>9</sup> Baker,<sup>10</sup> and ourselves.<sup>11</sup> It is significant that examples of such polyhedra are not observed for either the  $B_N H_N$  or  $B_N Cl_N$  types of cluster (with the exception of tetrahedral  $B_4 Cl_4$ ) presumably because the polar geometries result in

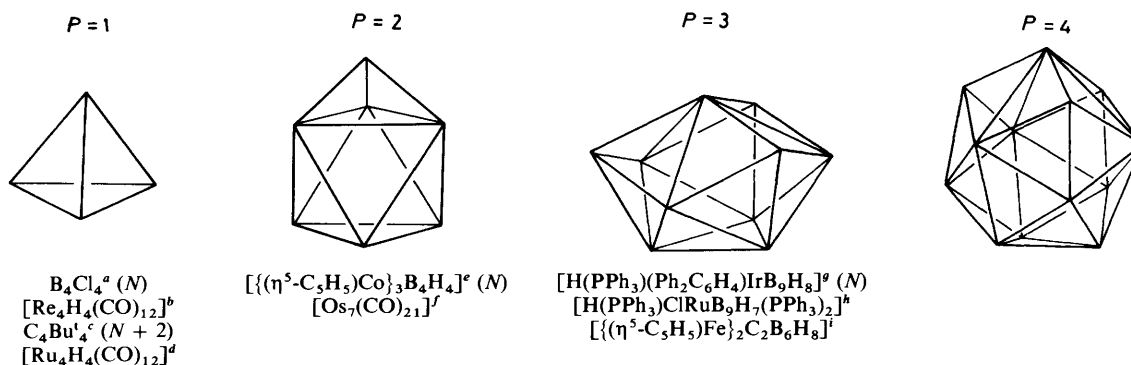


**Figure 2.** Examples of  $C_3$  polar deltahedra [with three-fold rotational symmetry and  $(3P + 1)$  atoms]. References: <sup>a</sup> M. Atoji and W. N. Lipscomb, *Acta Crystallogr.*, 1953, **6**, 547. <sup>b</sup> R. Saillant, G. Barcelo, and H. D. Kaesz, *J. Am. Chem. Soc.*, 1970, **92**, 5739. <sup>c</sup> G. Maier, S. Pfriem, U. Schafter, and R. Matusch, *Angew. Chem.*, 1978, **90**, 652. <sup>d</sup> R. D. Wilson, S. M. Wu, R. A. Love, and R. Bau, *Inorg. Chem.*, 1978, **17**, 1271. <sup>e</sup> J. R. Pipal and R. N. Grimes, *Inorg. Chem.*, 1977, **16**, 3255. <sup>f</sup> C. R. Eady, B. F. G. Johnson, J. Lewis, R. Mason, P. B. Hitchcock, and K. M. Thomas, *J. Chem. Soc., Chem. Commun.*, 1977, 385. <sup>g</sup> Ref. 9a. <sup>h</sup> Ref. 9d. <sup>i</sup> K. P. Callahan, W. J. Evans, F. Y. Lo, C. E. Strouse, and M. F. Hawthorne, *J. Am. Chem. Soc.*, 1975, **97**, 296.

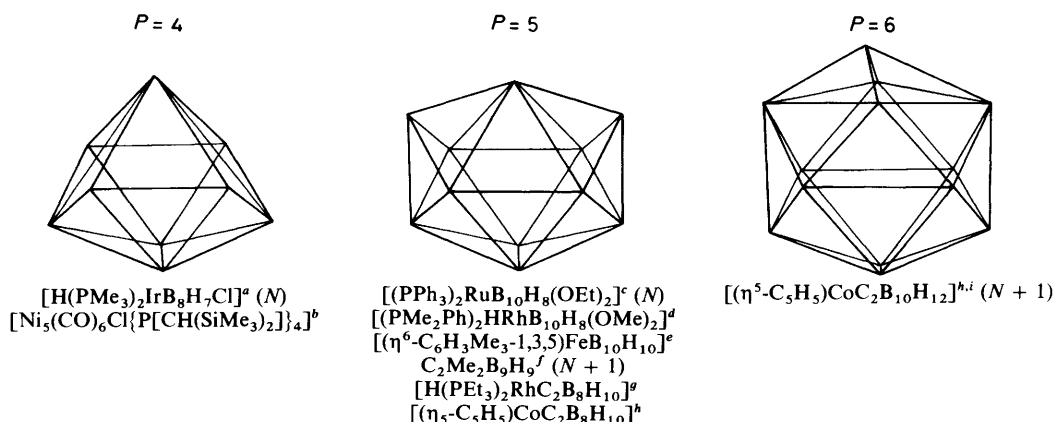
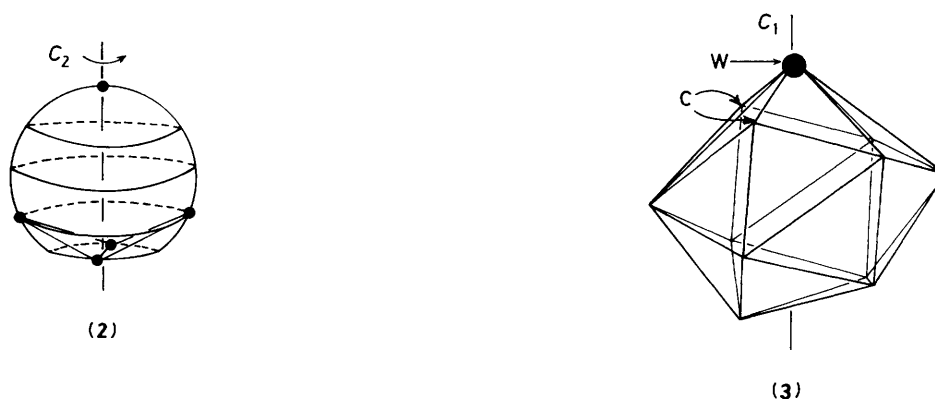


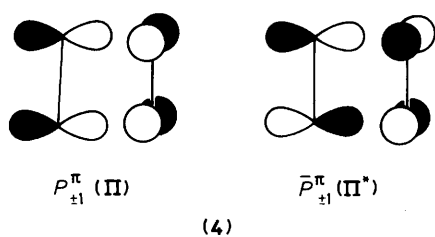
**Figure 3.** Examples of  $C_2$  polar deltahedra [with two-fold rotational symmetry and  $(2P + 1)$  atoms]. References: <sup>a</sup> J. Bould, N. N. Greenwood, J. D. Kennedy, and W. S. McDonald, *J. Chem. Soc., Dalton Trans.*, 1985, 1433. <sup>b</sup> M. M. Olmstead and P. P. Power, *J. Am. Chem. Soc.*, 1984, **106**, 1495. <sup>c</sup> Ref. 9d. <sup>d</sup> Ref. 9e. <sup>e</sup> R. P. Micciche, J. J. Briguglio, and L. G. Sneddon, *Inorg. Chem.*, 1984, **23**, 3992. <sup>f</sup> C. Tsai and W. Streib, *J. Am. Chem. Soc.*, 1966, **88**, 4513. <sup>g</sup> C. W. Jung and M. F. Hawthorne, *J. Am. Chem. Soc.*, 1980, **102**, 3024. <sup>h</sup> D. F. Dustin, W. J. Evans, C. J. Jones, R. J. Wiersma, H. Gong, S. Chen, and M. F. Hawthorne, *J. Am. Chem. Soc.*, 1974, **96**, 3085. <sup>i</sup> M. R. Churchill and B. G. DeBoer, *Inorg. Chem.*, 1974, **13**, 1411.



substantial charge asymmetries between the boron atoms. In isolobal clusters, however, the presence of atoms of either higher or lower electronegativities leads to a stabilisation of the polar deltahedral geometries if they are located in the appropriate sites. In particular the location of metal atoms at the high connectivity sites has a strong stabilising effect.

(ii)  $C_2$  Polar deltahedra. In this sub-class of polar deltahedra the polar axis passes at right angles through the mid-point of an edge of the deltahedron (2), making it a  $C_2$  axis. This leads to clusters with  $C_2$  or  $C_{2v}$  symmetry. Polar deltahedra with these

cluster symmetries are characterised by  $(2P + 1)$  atoms, where  $P$  represents the number of pairs of atoms disposed about the principal ( $C_2$ ) axis. As there are no  $E$  representations in  $C_2$  or  $C_{2v}$  symmetry there is no group theoretical restriction opposing the occurrence of clusters with  $(N + 1)$  skeletal electron pairs. Instead the electron count depends more critically on the frontier orbital spacings which in turn depend on the nature of the cluster fragments. In particular, calculations have shown<sup>12</sup> that with boron atoms in the polar sites an  $(N + 1)$  count is favoured while with metals in these sites either  $N$  or  $(N + 1)$

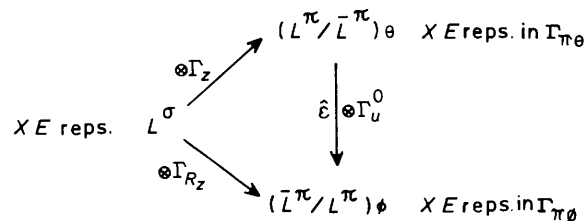


skeletal electron pairs is possible. Examples of polar deltahedral clusters with  $C_{2v}$  symmetry and  $N$  or  $(N + 1)$  skeletal electron pairs are shown in Figure 3.

(iii)  $C_1$  Polar deltahedra. In this sub-class of polar deltahedra the polar axis does not pass through the centroid of a face or the middle of an edge of the deltahedron, so that there is no rotational symmetry (only a  $C_1$  axis). This leads to clusters with either  $C_1$ ,  $C_s$ , or  $C_3$  symmetry. As for the  $C_2$  polar deltahedra, the lack of any  $E$  representations in these point groups means that clusters with  $N$  or  $(N + 1)$  skeletal electron pairs should be possible, depending on the nature of the atoms in the various cluster sites. The complex  $[\text{PtW}(\text{CO})_2(\text{PEt}_3)_2\{\eta^6\text{-C}_2\text{B}_9\text{H}_8\text{-(CH}_2\text{R)Me}_2\}](\text{R} = p\text{-tolyl})$ <sup>13</sup> is an example of such a cluster, having a 12-atom  $C_2\text{B}_9\text{W}$  cage, with  $C_s$  symmetry, (3), and  $12(N)$  skeletal electron pairs.

A more detailed analysis of the bonding in polar deltahedral clusters will be presented in a subsequent publication.<sup>12</sup>

**Class 3: Bipolar Deltahedra.**—Bipolar deltahedra have two atoms lying on the principal ( $C_n$ ) rotation axis, generating  $D_{nh}$  (e.g. bipyramidal) or  $D_{nd}$  (e.g. bicapped antiprismatic) structures. In such deltahedra the atoms form two subsets which lie on spherical shells of different radii. Following the analysis presented above for polar deltahedra the polar atoms are initially ignored and the  $L^\sigma$  orbitals of the component layers in the cluster are considered, combinations of these orbitals being taken to generate the  $L^\pi$  orbitals of the polyhedron (minus polar atoms). If the  $L^\sigma$  orbitals contain a certain number ( $X$ ) of  $E$  representations (reps.) then  $(L^\pi/\bar{L}^\pi)_\theta$  will also contain  $XE$  representations, as will  $(L^\pi/\bar{L}^\pi)_\phi$ , as shown below.



In total there are an even number ( $2X$ ) of  $E$  representations in the  $L^\pi/\bar{L}^\pi$  set. Considering the two polar atoms, in-phase ( $\Pi$ ) and out-of-phase ( $\Pi^*$ ) combinations of the  $p^\pi$  orbitals ( $p_x, p_y$ ) on each atom result, (4), corresponding to another two  $E$  representations. The  $L^\pi$  and  $\bar{L}^\pi$  orbitals of the bipolar cluster as a whole are generated by taking combinations of the orbitals of the polar atoms and of the remainder of the polyhedron. In total there is an even number ( $2X + 2$ ) of  $E$  representations within the  $L^\pi/\bar{L}^\pi$  manifold, which are split into  $(X + 1)$  bonding ( $L^\pi$ ) and  $(X + 1)$  antibonding ( $\bar{L}^\pi$ )  $E$  pairs. There is, therefore, no group theoretical restriction leading to a departure from the  $(N + 1)$  rule, so the majority of bipolar clusters obey the rule.

There are, however, a significant number of bipolar clusters which do not obey the  $(N + 1)$  rule. Deviations from the rule arise because bipolar clusters do not approximate closely enough to spherical. The nature of any deviation from the  $(N + 1)$  rule is best analysed in terms of the interaction between

the orbitals of the various sets of symmetry-equivalent cluster vertices, which may be regarded as lying on concentric spheres of differing radii. In the case of bipyramidal or bicapped antiprismatic clusters these two sets of atoms are the polar and the remaining (non-polar) atoms which either lie on the equator ( $D_{nh}$ ) or are related by an improper rotation axis  $S_{2n}$  ( $D_{nd}$ ).

Since the two polar atoms are not within bonding distance the spread of  $L^\pi$  and  $\bar{L}^\pi$  orbitals (i.e.  $P_{\pm 1}^\pi$  and  $\bar{P}_{\pm 1}^\pi$ ) for these atoms is much narrower than for the non-polar atoms. The  $P_{\pm 1}^\pi$  and  $\bar{P}_{\pm 1}^\pi$  linear combinations of the polar atoms can only interact with the  $L_{\pm 1}^\pi$  and  $\bar{L}_{\pm 1}^\pi$  orbitals of the rest of the cluster (ring or antiprism). Two slightly different situations apply for bicapped rings (bipyramids,  $D_{nh}$ ) and bicapped antiprisms ( $D_{nd}$ ) and these are illustrated in Figures 4 and 5.

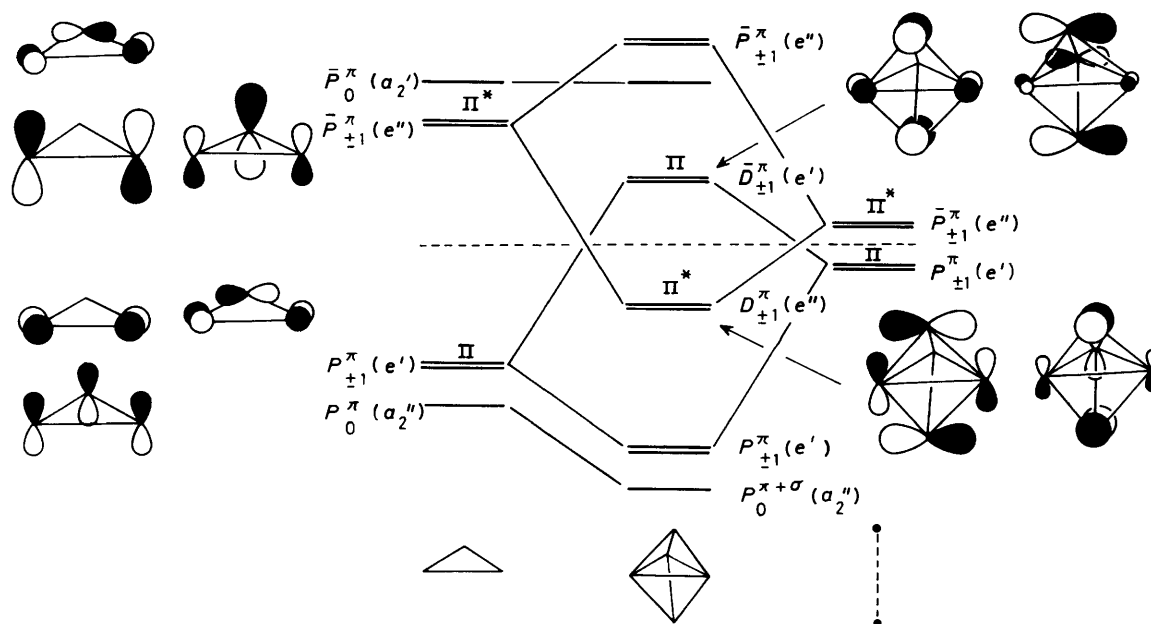
(i) **Bipyramidal clusters** ( $D_{nh}$ ). Figure 4(a) shows the polar/non-polar interaction diagram for a trigonal bipyramidal cluster. The  $\bar{P}_{\pm 1}^\pi$  ( $\Pi^*$ ) polar combination is stabilised by the more strongly antibonding  $\bar{P}_{\pm 1}^\pi$  pair of the ring, yielding a weakly bonding  $e''$  pair ( $D_{\pm 1}^{\pi''}$ ) with a dominant ( $\Pi^*$ ) polar-atom contribution. In a similar fashion the  $P_{\pm 1}^\pi$  ( $\Pi$ ) polar combination is destabilised by the more strongly bonding  $P_{\pm 1}^\pi$  orbitals of the ring, thereby generating a weakly antibonding (parity related)  $e'$  pair ( $\bar{D}_{\pm 1}^{\pi'}$ ) also with a dominant ( $\Pi$ ) polar-atom contribution.

The pentagonal bipyramid shows many of the same features as those described above if the polar and equatorial atoms are approximately equidistant from the centre of the cluster, but some additional electronic effects arise if the polar atoms are displaced by large distances towards the centre of the polyhedron. Since the pentagonal ring is larger than the trigonal ring the polar atoms must move closer to the centre of the cluster to equalise all the skeletal bond lengths. We will discuss the situation for small displacements of the polar atoms first. A stronger interaction occurs between the  $P^\pi/\bar{P}_{\pm 1}^\pi$  orbitals of the polar atoms and the orbitals of the ring than in the trigonal bipyramidal case, because the  $\bar{P}_{\pm 1}^\pi$  orbitals are now weakly bonding (indeed they correspond to the h.o.m.o.s in  $[\text{C}_5\text{H}_5]^-$ ). The resulting  $D_{\pm 1}^{\pi''}$  ( $e_1''$ ) orbitals of the pentagonal bipyramid are therefore no longer necessarily the h.o.m.o.s. Calculations have indicated that they lie close in energy to the  $D_{\pm 2}^{\pi''}$  ( $e_2''$ ) orbitals (5) which are localised exclusively on the ring atoms. The latter may therefore become the h.o.m.o.s in the example  $[\text{B}_7\text{H}_7]^{2-}$ . The ordering of the antibonding  $\bar{D}_{\pm 1}^{\pi'}$  ( $e_1'$ ) and  $\bar{D}_{\pm 2}^{\pi'}$  ( $e_2'$ ) orbitals is also going to be sensitive to small changes in internuclear distances and electronic effects.

Such minor differences apart these bipyramidal clusters are characterised by parity related  $D^\pi$  and  $\bar{D}^\pi$  orbitals of  $e'$  and  $e''$  symmetry in the frontier orbital region as long as the polar atoms do not interact strongly. These arguments are also applicable to hexagonal bipyramidal clusters, although in this instance the frontier orbitals have  $e_g$  and  $e_u$  symmetry. Bipyramidal clusters (with appropriate atom substitutions) are therefore capable of supporting  $(N - 1)$ ,  $(N + 1)$ , and  $(N + 3)$  skeletal electron pairs, although to date the only example of a bipyramidal cluster with  $(N - 1)$  skeletal electron pairs is  $[\{\text{V}(\eta^5\text{-C}_5\text{H}_5)_2\}_2(\mu\text{-C}_6\text{H}_6)]$  which has a hexagonal bipyramidal structure.<sup>14</sup> Examples of bipyramidal clusters with  $(N + 1)$  and  $(N + 3)$  skeletal electron pairs are given in Table 1.

In those situations where the distance between the polar atoms approaches the sum of the covalent radii then the generalisation developed above has to be modified to incorporate the additional strong interactions which arise. Most importantly the  $P_0^{\sigma+\pi}$  orbital [illustrated in Figure 4(b)] is destabilised significantly, because of the strong antibonding interactions between the polar atoms and can enter into the frontier orbital region. If the antibonding interactions are particularly strong then an  $N$  electron pair situation may become favourable. Fowler<sup>4</sup> has suggested that this situation may apply to  $\text{B}_7\text{Br}_7$ ,

(a)

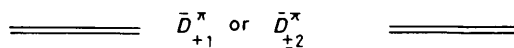


(b)

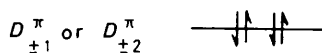
Possible skeletal electron pair counts

$(N-1), (N+1), (N+3)$

$(N), (N+1), (N+3)$



----- Non-bonding level



h.o.m.o.s for  $(N+1)$  skeletal electron pair cluster

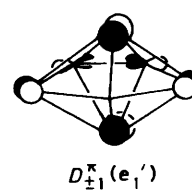
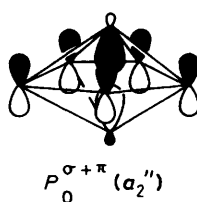
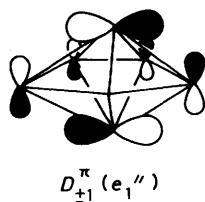


**Figure 4.** Frontier orbital patterns for bipyramidal clusters. (a) Interaction between the  $L^*$  and  $\bar{L}^*$  orbitals of the ring and polar atoms of a trigonal bipyramidal ( $D_{3h}$ ) cluster. (b) Possible frontier orbital patterns for pentagonal bipyramidal ( $D_{5h}$ ) clusters

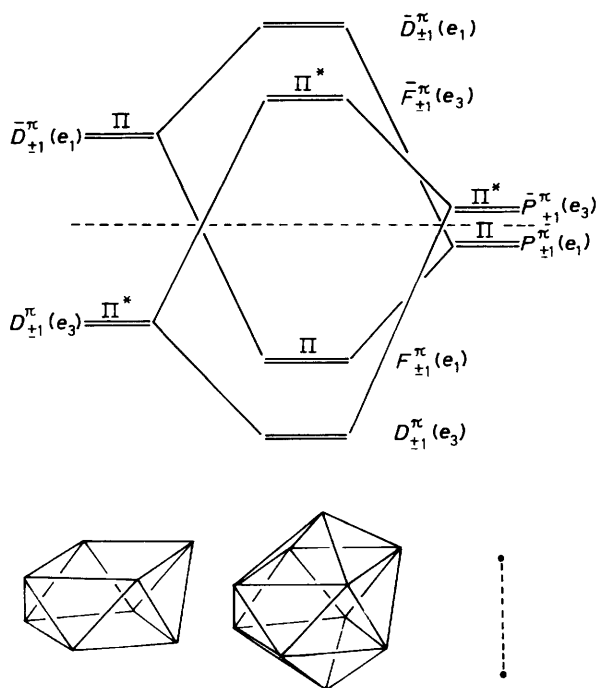


Figure 5. Interaction of the  $L^*$  and  $\bar{L}^*$  orbitals of the polar and non-polar atoms of a bicapped square antiprismatic cluster ( $D_{4d}$ )

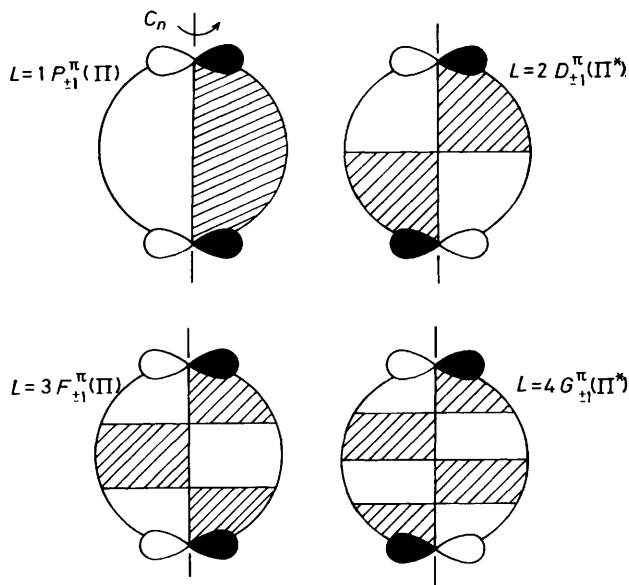
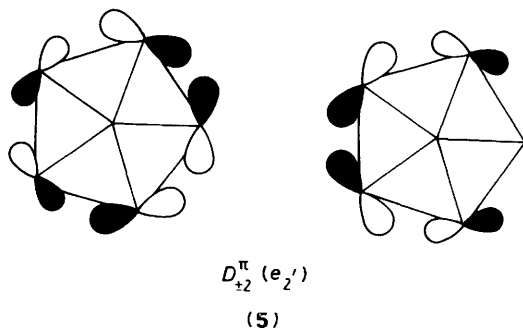


Figure 6. Variation of  $L$  (number of angular modes in the cluster wavefunction) of the nodal characteristics (with respect to the polar atoms of a bipolar cluster) of  $L_{\pm 1}^{\pi}$

which is diamagnetic. Figure 4(b) summarises the alternative patterns of frontier orbitals for pentagonal bipyramids, which are influenced primarily by the relative displacements of the polar and equatorial atoms.

(ii) *Bicapped antiprismatic clusters* ( $D_{nd}$ ). The frontier orbitals of the square antiprism, shown on the left hand side of Figure 5, are  $D_{\pm 1}^{\pi}/\bar{D}_{\pm 1}^{\pi}$  rather than  $P_{\pm 1}^{\pi}/\bar{P}_{\pm 1}^{\pi}$  due to the extra layer of atoms present (though, with respect to each of the open faces these functions are singly noded, like  $P_{\pm 1}^{\pi}/\bar{P}_{\pm 1}^{\pi}$  in the ring case). Because of the extra node (perpendicular to the principal rotation axis) the  $D_{\pm 1}^{\pi}$  pair have  $\Pi^*$  rather than  $\Pi$  character with respect to the polar atoms. Figure 6 shows schematically how the nodal properties (with respect to the polar atoms) of  $L_{\pm 1}^{\pi}$  vary with  $L$ . In general  $L_{\pm 1}^{\pi}$  orbitals possess  $\Pi$  symmetry with respect to the polar atoms for  $L = 2n + 1$  (i.e.  $L$  odd) and  $\Pi^*$  for  $L = 2n$  (i.e.  $L$  even). The parity inversion operation reverses bonding characteristics so, for example, if  $L_{\pm 1}^{\pi}$  have  $\Pi$  character with respect to the polar atoms then  $\bar{L}_{\pm 1}^{\pi}$  will have  $\Pi^*$  character.

Interaction of the  $P_{\pm 1}^{\pi}$  ( $\Pi$ ) and  $\bar{P}_{\pm 1}^{\pi}$  ( $\Pi^*$ ) orbitals of the polar atoms with the  $D_{\pm 1}^{\pi}/\bar{D}_{\pm 1}^{\pi}$  orbitals of the antiprism (as depicted in Figure 5) generates a bonding pair  $F_{\pm 1}^{\pi}$  ( $\Pi$ ) and an antibonding pair  $\bar{F}_{\pm 1}^{\pi}$  ( $\Pi^*$ ) which are predominantly localised on the polar atoms, (6). Thus the h.o.m.o.s and lowest unoccupied molecular orbitals (l.u.m.o.s), as for the bipyramids discussed

Table 1. Bipyramidal clusters

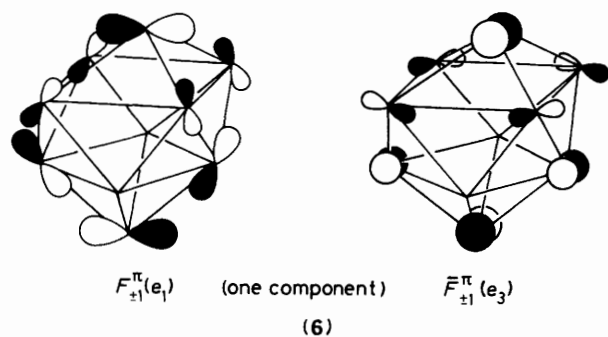
Cluster	Skeletal electron pairs	Ref.
(a) Trigonal bipyramidal		
$C_2B_3H_5$	$6(N + 1)$	<i>a</i>
$[Os_5(CO)_{16}]$	6	<i>b</i>
$[Sn_5]^{2-}$	6	<i>c</i>
$[Ni_5(CO)_{12}]^{2-}$	$8(N + 3)$	<i>d</i>
$[Rh_5(CO)_{14}]^{2-}$	8	<i>e</i>
(b) Pentagonal bipyramidal		
$[B_5H_7]^{2-}$	$8(N + 1)$	<i>f</i>
$[(CO)_5FeC_2B_4H_6]$	8	<i>g</i>
$[(\eta^5-C_5H_5)Co(MeC_2B_3H_4)-Co(\eta^5-C_5H_5)]$	8	<i>h</i>
$[(\eta^5-C_5H_5)Ni(\mu-C_5H_5)-Ni(\eta^5-C_5H_5)]$	$10(N + 3)$	<i>i</i>

<sup>a</sup> R. E. Williams, *Adv. Inorg. Chem. Radiochem.*, 1976, **18**, 67. <sup>b</sup> C. R. Eady, B. F. G. Johnson, J. Lewis, B. E. Reichert, and G. M. Sheldrick, *J. Chem. Soc., Chem. Commun.*, 1976, 271. <sup>c</sup> P. A. Edwards and J. D. Corbett, *Inorg. Chem.*, 1977, **16**, 903. <sup>d</sup> G. Longoni, P. Chini, L. D. Lower, and L. F. Dahl, *J. Am. Chem. Soc.*, 1975, **97**, 5034. <sup>e</sup> S. Martinengo, G. Ciani, and A. Sironi, *J. Chem. Soc., Chem. Commun.*, 1979, 1059. <sup>f</sup> W. N. Lipscomb, 'Boron Hydrides', Benjamin, New York, 1963. <sup>g</sup> R. N. Grimes, *J. Am. Chem. Soc.*, 1971, **93**, 261. <sup>h</sup> D. C. Beer, V. R. Miller, L. G. Sneddon, R. N. Grimes, M. Mathew, and G. J. Palenik, *J. Am. Chem. Soc.*, 1973, **95**, 3046. <sup>i</sup> A. Salzer and H. Werner, *Angew. Chem., Int. Ed. Engl.*, 1978, **17**, 869.

above, are both doubly degenerate ( $E$ ) molecular orbitals. As for the bipyramidal clusters this gives rise, in principle, to the possibility of clusters with  $(N - 1)$ ,  $(N + 1)$ , or  $(N + 3)$  skeletal electron pairs. However, on comparing the orbital interaction diagrams for the trigonal bipyramid and bicapped antiprisms [Figures 4(a) and 5] more closely it may be seen that the h.o.m.o.-l.u.m.o. separation is greater in the latter case. This arises because the  $\Pi^*$  orbitals of the polar atoms interact with strongly bonding orbitals ( $D_{\pm 1}^{\pi}$ ) rather than antibonding ones ( $\bar{P}_{\pm 1}^{\pi}$ ). The result of this is to make the occurrence of bicapped antiprismatic clusters with  $(N + 3)$  skeletal electron pairs less

favourable on energy grounds and, to date, no such clusters have been isolated [( $N - 1$ ) electron pair clusters would have  $F_{\pm 1}^{\pi}$  unpopulated which is also unfavourable because these orbitals have considerable bonding character].

**Class 4: Non-polar Deltahedra.**—Non-polar deltahedra are also non-spherical, with the cluster atoms generally lying on the surfaces of two spheres with different radii. As the name suggests these polyhedra do not possess any atoms on the principal rotation axis, but instead have a ring (planar or puckered) of atoms around the equator of the cluster. It has been shown above that, for a group of atoms where no atoms lie on the principal rotation axis, the  $L^{\pi}/\bar{L}^{\pi}$  orbitals contain an even number of  $E$  representations. Non-polar clusters cannot, therefore, have their h.o.m.o. and l.u.m.o. as a degenerate pair, so there is no symmetry induced breaking of the ( $N + 1$ ) rule. As for bipolar clusters, deviations from the ( $N + 1$ ) rule must be rationalised in terms of interactions between the  $L^{\pi}$  and  $\bar{L}^{\pi}$  orbitals of the two subsets of atoms (equatorial or non-equatorial).



(i)  $D_{3h}$  Planar equatorial. The tricapped trigonal prism possesses three atoms which lie on the equatorial plane and are related by a  $C_3$  axis. The cluster has a mirror plane of symmetry passing through the equator and therefore has overall  $D_{3h}$  symmetry. Larger clusters may be envisaged which also have this symmetry, but it is not possible to have non-polar deltahedral clusters with  $D_{nh}$  symmetry and  $n > 3$  since this would lead to (open) non-triangular faces.

On the right-hand side of Figure 7 the  $L^{\pi}$  and  $\bar{L}^{\pi}$  orbitals of a three-membered ring are illustrated. The  $P^{\pi}$  and  $\bar{P}^{\pi}$  molecular orbitals of this subset of atoms interact with the molecular orbitals of the trigonal prism. As Figure 7 shows, the  $e'$  and  $e''$  components ( $P_{\pm 1}^{\pi}/\bar{P}_{\pm 1}^{\pi}$ ) interact with the non-bonding  $\bar{D}_{\pm 1}^{\pi}$  ( $e'$ )

Table 2. Tricapped trigonal prismatic clusters

Cluster	Skeletal electron pairs	Ref.
$B_3Cl_9$	9 ( $N$ )	a
$[B_9H_9]^{2-}$	10 ( $N + 1$ )	b
$[Ge_9]^{2-}$	10	c
$[TiSn_8]^{3-}$	10	d
$[(\eta^5-C_5H_5)CoC_2B_6H_8]$	10	e
$[(PMe_3)_2PtC_2B_6H_8]$	10	f
$[Bi_9]^{5+}$	11 ( $N + 2$ )	g

<sup>a</sup> M. B. Hursthouse, J. Kane, and A. G. Massey, *Nature (London)*, 1970, **228**, 659. <sup>b</sup> L. J. Guggenberger, *Inorg. Chem.*, 1968, **7**, 2260. <sup>c</sup> C. H. E. Belin, J. D. Corbett, and A. Cisar, *J. Am. Chem. Soc.*, 1977, **99**, 7163. <sup>d</sup> R. C. Burns and J. D. Corbett, *J. Am. Chem. Soc.*, 1982, **104**, 2804. <sup>e</sup> D. F. Dustin, W. J. Evans, C. J. Jones, R. J. Wiersma, H. Gong, S. Chan, and M. F. Hawthorne, *J. Am. Chem. Soc.*, 1973, **95**, 4565. <sup>f</sup> A. J. Welch, *J. Chem. Soc., Dalton Trans.*, 1976, 225. <sup>g</sup> R. M. Friedman and J. D. Corbett, *Inorg. Chem.*, 1973, **12**, 1134.

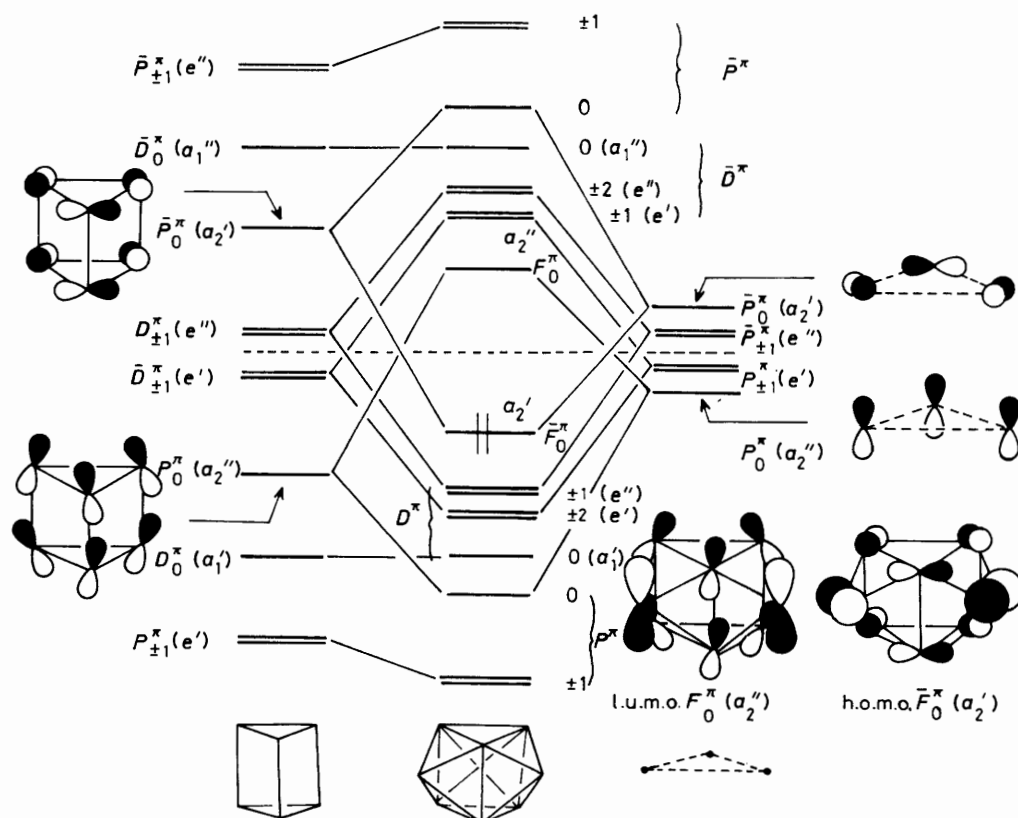


Figure 7. Interaction of the  $L^{\pi}$  and  $\bar{L}^{\pi}$  orbitals of the two subsets of atoms forming a tricapped prismatic cluster ( $D_{3h}$ )

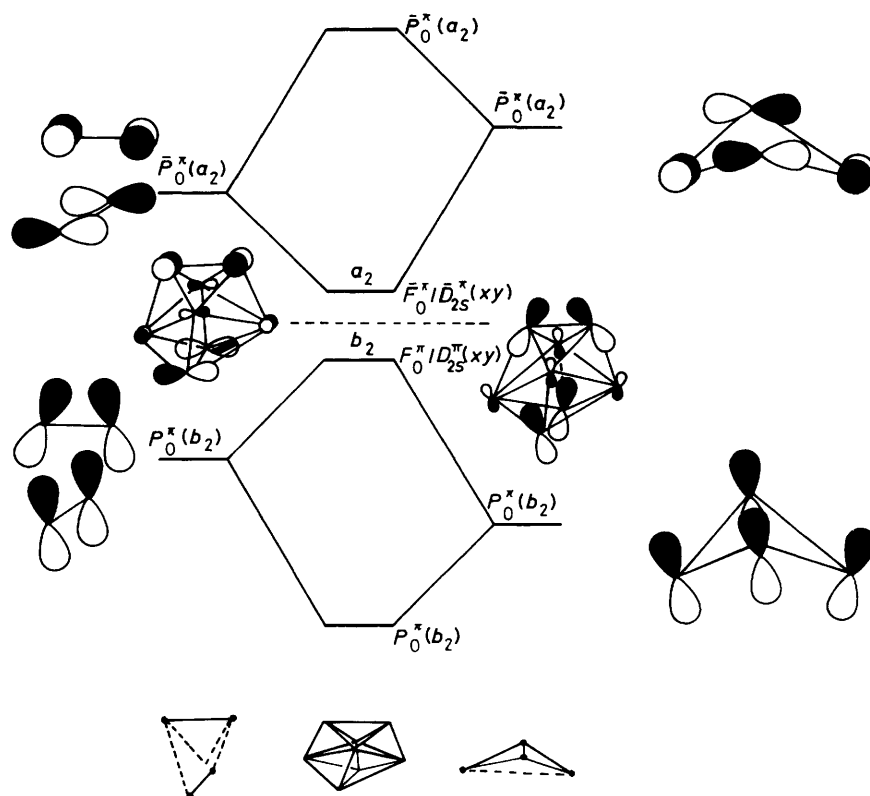
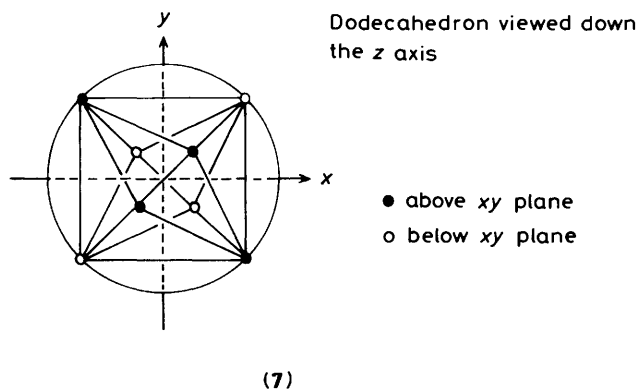


Figure 8. Interaction of the  $L^*$  and  $\bar{L}^*$  orbitals of the two subsets of atoms forming a triangular dodecahedral cluster ( $D_{2d}$ )



and  $D_{\pm 1}^*$  ( $e''$ ) orbitals of the trigonal prism to generate strongly bonding and antibonding combinations. In contrast the  $a_2''$  and  $a_2'$  components ( $P_0^*/\bar{P}_0^*$ ) interact with more strongly bonding or antibonding orbitals of the trigonal prism (see Figure 7) to generate one weakly antibonding orbital ( $F_0^*$ ,  $a_2''$ ) and one weakly bonding orbital ( $\bar{F}_0^*$ ,  $a_2'$ ). Consequently the frontier orbitals of the non-polar deltahedron consist of a parity related pair of (non-degenerate) orbitals derived from  $P_0^*$  and  $\bar{P}_0^*$ , which are predominantly localised on the equatorial atoms. Interestingly, Stone's conclusions for deltahedral boranes ( $L^*$  bonding and  $\bar{L}^*$  antibonding) break down in this case because the h.o.m.o. has odd parity ( $\bar{F}_0^*$ ) and the l.u.m.o. has even parity ( $F_0^*$ ).<sup>15</sup> This cluster geometry is therefore capable of accommodating  $N$ ,  $(N + 1)$ , or  $(N + 2)$  skeletal electron pairs.<sup>16</sup> Examples of boranes, main-group clusters, and metallocarboranes with nine vertex atoms and these alternative electron counts are summarised in Table 2.

(ii)  $D_{nd}$  Puckered equatorial. The deltahedral dodecahedron

( $N = 8$ ) has a puckered arrangement of four atoms around the equator. The polyhedron has  $D_{2d}$  symmetry and the equatorial atoms are related by an  $S_4$  axis (in general an  $S_{2n}$  axis would relate the  $2n$  equatorial atoms of a  $D_{nd}$  cluster). Larger clusters of  $D_{2d}$  or  $D_{3d}$  symmetry would fall into this class, but it is not possible [for the reasons mentioned in class 4(i)] to have non-polar deltahedral clusters with  $D_{nd}$  symmetry and  $n > 3$ .

As for the tricapped trigonal prism, the frontier orbitals of the dodecahedron arise from the interaction of the  $P_0^*$  and  $\bar{P}_0^*$  orbitals (see Figure 8) of the two subsets of atoms. The two subsets, in this case, may both be considered as distorted tetrahedra.<sup>17</sup> The four equatorial atoms may be regarded as constituting a flattened tetrahedron. In contrast to the tricapped trigonal prism these equatorial atoms are within bonding distance of each other, which has the effect of making their  $P_0^*$  combination quite strongly bonding and their  $\bar{P}_0^*$  combination quite strongly antibonding. In this case the connectivities of the non-equatorial atoms (elongated tetrahedron) are lower than the equatorial ones so the spread of  $L^*$  and  $\bar{L}^*$  orbitals is narrower for these non-equatorial atoms. As Figure 8 shows, this results in the (weakly bonding) h.o.m.o. and (weakly antibonding) l.u.m.o. being predominantly localised on the non-equatorial vertices, in contrast to the tricapped trigonal prism. Figure 8 also shows that the h.o.m.o. is of  $b_2$  symmetry and may be identified as  $F_0^*$  and the (parity related) l.u.m.o. is of  $a_2$  symmetry and may be described as  $\bar{F}_0^*$ . The h.o.m.o. and l.u.m.o. may be alternatively described as  $D_{2s}^*(xy)$  and  $\bar{D}_{2s}^*(xy)$  respectively [the axis system is depicted in (7)] since these functions are identical to  $F_0^*/\bar{F}_0^*$  for the  $D_{2d}$  dodecahedron. The advantage of the  $F_0^*/\bar{F}_0^*$  notation is that it emphasises the similarity to the tricapped trigonal prism and also explains why the frontier orbitals are weakly bonding or antibonding whereas the remainder of the  $D^*$  and  $\bar{D}^*$  functions are strongly bonding and antibonding respectively.<sup>17,18</sup> Due to the weakly bonding and



**Table 3.** (Triangulated) dodecahedral clusters

Cluster	Skeletal electron pairs	Ref.
$B_8Cl_8$	8 ( $N$ )	<i>a</i>
$\{(\eta^5-C_5H_5)Co\}_4B_4H_4$	8	<i>b</i>
$[B_8H_8]^{2-}$	9 ( $N + 1$ )	<i>c</i>
$[(\eta^5-C_5H_5)CoSnC_2B_4Me_2H_4]$	9	<i>d</i>
$\{(\eta^5-C_5H_5)Ni\}_4B_4H_4$	10 ( $N + 2$ )	<i>e</i>

<sup>a</sup> R. A. Jacobson and W. N. Lipscomb, *J. Chem. Phys.*, 1959, **31**, 605. <sup>b</sup> J. R. Pipal and R. N. Grimes, *Inorg. Chem.*, 1979, **18**, 257. <sup>c</sup> L. J. Guggenberger, *Inorg. Chem.*, 1969, **8**, 2771; F. Klanberg, D. R. Eaton, L. J. Guggenberger, and E. L. Muetterties, *ibid.*, 1967, **6**, 1271. <sup>d</sup> K. S. Wong and R. N. Grimes, *Inorg. Chem.*, 1977, **16**, 2053. <sup>e</sup> J. R. Bowser, A. Bonny, J. R. Pipal, and R. N. Grimes, *J. Am. Chem. Soc.*, 1979, **101**, 6229.

antibonding nature of the non-degenerate h.o.m.o. and l.u.m.o. the triangular dodecahedron (like the tricapped trigonal prism) can accommodate  $N$ , ( $N + 1$ ), or ( $N + 2$ ) skeletal electron pairs.<sup>17</sup> Examples of such clusters are given in Table 3. For both the dodecahedron and the tricapped trigonal prism the stabilisation of  $N$  skeletal electron pair clusters by terminal halide ligands (e.g.  $B_8Cl_8$  and  $B_8I_8$ ) has been attributed to the h.o.m.o. being raised in energy due to  $\pi$  interaction with the ligands.<sup>19</sup>

### Conclusions

The detailed analysis presented above for the four classes of deltahedral cluster can be summarised effectively in terms of the following generalisations derived from group theory and the parity transformation inherent in Stone's Tensor Surface Harmonic Analysis.

(a) *Centrosymmetric Spherical Clusters.*—The presence of a centre of symmetry in such clusters prevents the occurrence of any self-conjugate representations. In addition the highly spherical nature of these clusters ensures that the tangential orbitals are split into strongly bonding ( $L^*$ ) and strongly antibonding ( $\bar{L}^*$ ) components, so that the ( $N + 1$ ) rule is rigorously obeyed.

(b) *Polar Deltahedral Clusters.*—Polar deltahedral clusters with  $C_{3v}$  symmetry possess an odd number of  $E$  representations, leading to the occurrence of a non-bonding (self-conjugate)  $E$  pair  $[(L^*/\bar{L}^*)_{\pm 1}]$  of orbitals which are predominantly localised on the polar atom. The ( $N + 1$ ) rule is broken because the degenerate frontier orbitals give rise to closed shell configurations for  $N$  and ( $N + 2$ ) skeletal electron pairs.

(c) *Bipolar and Non-polar Clusters.*—These clusters consist of two subsets of atoms which lie on the surfaces of concentric spheres of different radii (bispherical deltahedra). This deviation from spherical topology leads to a spectrum of molecular orbitals intermediate between those anticipated from Stone's particle on a sphere solution and those of the individual subsets, each of which are solutions to the particle on a sphere problem. If the problem is analysed in terms of the interactions between the two subsets (which may be termed the inner and outer spheres) then the parity transformation is helpful in deciding the symmetries of the frontier orbitals.

In the point groups  $D_{(2n+1)d}$  and  $D_{nh}$  there are no self-conjugate representations<sup>4</sup> and in the former case even- and odd-parity functions are distinguished by their differing

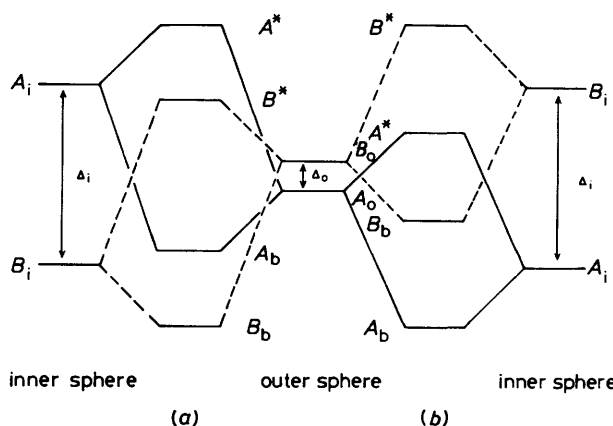


**Figure 9.** The alternative ways in which frontier orbitals of two subsets of atoms may interact to give the orbitals of a bispherical cluster

behaviour ( $g$  or  $u$ ) under inversion while in the latter case they are distinguished by their differing symmetries (' or ") with respect to the mirror plane ( $\sigma_h$ ) [equations (4) and (5)].

$$L^*(g,u) \xrightarrow{\otimes \Gamma_o^g} \bar{L}^*(u,g) \quad (4)$$

$$L^*(',") \xrightarrow{\otimes \Gamma_o^g} \bar{L}^*(",') \quad (5)$$

Figure 9 illustrates the interaction between a pair of parity related sets of orbitals ( $A$  and  $B$ , with symmetries  $\Gamma_A$  and  $\Gamma_B$ ) on the inner sphere and a similar pair of outer sphere orbitals. The spread of orbitals is narrower for the outer sphere because the atoms are generally further apart on the outer sphere. The parity transformation requires that the molecular orbitals of the bispherical cluster are also symmetrically disposed about the non-bonding line. The interaction between orbitals  $A_i$  (inner) and  $A_o$  (outer) generates a bonding combination ( $A_b$ ) and an antibonding combination ( $A^*$ ). Similarly the  $B$  orbitals interact to form  $B_b$  and  $B^*$ . The parity transformation interchanges  $A$  and  $B$  and also reverses the bonding character of the orbitals as shown by (6) and (7). Orbitals  $A_b$

$$A_b \xleftrightarrow{\hat{\epsilon}} B^* \quad (6)$$

$$B_b \xleftrightarrow{\hat{\epsilon}} A^* \quad (7)$$

and  $B_b$  are no longer related by the parity transformation. Although the components from the inner and outer spheres in these molecular orbitals undergo parity inversion the interactions between the two spheres is bonding for both  $A_b$  and  $B_b$ . Physically this corresponds to a rotation of  $90^\circ$  (about a radial axis) of each  $p^n$  component on the inner sphere and an equal rotation in the opposite sense of the orbitals on the outer sphere. This operation, though having the same symmetry as the parity transformation operation is clearly distinct as it does not reverse the inner sphere–outer sphere bonding nature of the orbital. The same argument applies to the antibonding orbitals  $A^*$  and  $B^*$ .

Two alternative situations can be analysed from Figure 9 since the ordering of orbitals  $A$  and  $B$  on the inner sphere may either be the same as for the outer sphere or may be inverted. In Figure 9(a) the  $A$  orbital of the outer sphere and the  $B$  orbital of the inner sphere are bonding and a large h.o.m.o.–l.u.m.o. separation results for the bispherical cluster. In Figure 9(b), however, the  $A$  orbitals of both the outer and the inner spheres are bonding and a small h.o.m.o.–l.u.m.o. separation results. The magnitude of the h.o.m.o.–l.u.m.o. gap is found to be inversely related to the magnitude of the  $A$ – $B$  spacings ( $\Delta_i$  and  $\Delta_o$ ) for the inner and outer spheres. The Figure also shows that

**Table 4.** Outer sphere components of the frontier orbitals of bipolar and non-polar deltahedral clusters

Cluster class	Bipolar		Non-polar	
	$D_{nh}$	$D_{nd}$	$D_{nh}$	$D_{nd}$
Symmetry				
l.u.m.o.	$P_{\pm 1}^n$	$\bar{P}_{\pm 1}^n$	$P_0^n$	$\bar{P}_0^n$
h.o.m.o.	$\bar{P}_{\pm 1}^n$	$P_{\pm 1}^n$	$\bar{P}_0^n$	$P_0^n$

**Table 5.** Symmetries of cluster  $P^n$  and  $\bar{P}^n$  orbitals in some  $D_{nh}$  and  $D_{nd}$  point groups

	$D_{nh}$				$D_{nd}$			
	$n = 3$	4	5	6	2	3	4	5
$P_0^n$	$a_2''$	$a_{2u}$	$a_2''$	$a_{2u}$	$b_2$	$a_{2u}$	$b_2$	$a_{2u}$
$P_{\pm 1}^n$	$e'$	$e_u$	$e_1'$	$e_{1u}$	$e$	$e_u$	$e_1$	$e_{1u}$
$\bar{P}_0^n$	$a_2'$	$a_{2g}$	$a_2'$	$a_{2g}$	$a_2$	$a_{2g}$	$a_2$	$a_{2g}$
$\bar{P}_{\pm 1}^n$	$e''$	$e_g$	$e_1''$	$e_{1g}$	$e$	$e_g$	$e_3$	$e_{1g}$

the h.o.m.o. and l.u.m.o. are predominantly localised on the outer sphere for both situations.

In the class of bipolar deltahedral clusters the orbitals  $A$  and  $B$  are doubly degenerate  $E$  functions with the symmetries of the  $P_{\pm 1}^n$  and  $\bar{P}_{\pm 1}^n$  orbitals of the polar atoms. Bicapped antiprisms and trigonal bipyramids have been shown to belong to the cases illustrated in Figure 9(a) and (b) respectively. This explains the larger h.o.m.o.–l.u.m.o. separation in bicapped square antiprismatic clusters and the fact that the  $(N + 1)$  rule is adhered to for these clusters. On the other hand the h.o.m.o.–l.u.m.o. spacing in trigonal bipyramidal clusters is quite small and clusters with  $(N + 3)$  skeletal electron pairs have been characterised. The pentagonal bipyramid differs from the trigonal bipyramid in that its polar atoms lie on the inner rather than the outer sphere. The exact nature of the frontier orbitals in these clusters is very dependent on the relative ratios of the two sphere radii and the exact nature of the cluster and ligand atoms. The l.u.m.o.s are always doubly degenerate ( $\bar{D}_{\pm 1}^n$  or  $\bar{D}_{\pm 2}^n$ ) whereas the h.o.m.o.s may be either non-degenerate ( $P_0^n$ ) or doubly degenerate ( $D_{\pm 1}^n$  or  $D_{\pm 2}^n$ ). Since the h.o.m.o.–l.u.m.o. gap is generally small, skeletal electron pair counts ranging from  $(N - 1)$  to  $(N + 3)$  [excepting  $(N + 2)$ ] are possible. Similar arguments apply to bipyramidal clusters with six or more atoms in the equatorial plane.

The non-polar clusters (tricapped trigonal prism or dodecahedron) belong to the situation illustrated in Figure 9(b). In this case the orbitals  $A$  and  $B$  are singly degenerate, corresponding to the  $P_0^n$  and  $\bar{P}_0^n$  orbitals of the outer sphere. In the dodecahedron the spacing between the  $A$  and  $B$  orbitals for both spheres is sufficiently large for there to be no cross-over between the bonding component of the  $B$ – $B$  interaction ( $B_b$ ) and the antibonding component of the  $A$ – $A$  interaction ( $A^*$ ). Non-planar clusters (planar-equatorial or puckered-equatorial) may therefore accommodate  $N$ ,  $(N + 1)$ , or  $(N + 2)$  skeletal electron pairs.

Table 4 summarises the frontier orbital nature of bipyramidal and non-polar deltahedral clusters in terms of the orbitals of the outer sphere. In both of these classes of cluster the frontier orbitals are derived from components of the  $P^n$  and  $\bar{P}^n$  orbitals of the outer sphere. For bipolar clusters these components are  $P_{\pm 1}^n$  and  $\bar{P}_{\pm 1}^n$ , while for non-polar clusters they are  $P_0^n$  and  $\bar{P}_0^n$ , so a complementary pattern exists between the frontier orbital pattern of bipolar and non-polar deltahedral clusters. This Table also illustrates that for  $D_{nh}$  clusters (bipyramidal and non-polar planar equatorial) the ordering is  $B$  below  $A$ , that is the h.o.m.o. has  $\bar{P}^n$  character (outer sphere) and the l.u.m.o. has  $P^n$

character. In contrast  $D_{nd}$  clusters (bicapped antiprismatic and non-polar dodecahedral) have this ordering reversed. The symmetries of  $P^n$  and  $\bar{P}^n$  orbitals, for several  $D_{nh}$  and  $D_{nd}$  point groups, are listed in Table 5.

The arguments developed above are equally applicable to the large ( $N > 12$ ) deltahedral clusters discussed by Lipscomb and co-workers<sup>20</sup> provided that they do not deviate too greatly from spherical topology. Thus the degeneracies and number of nodes in a plane perpendicular to the principal rotation axis (*i.e.*  $M_L$  quantum numbers) of the frontier orbitals should be the same for these large clusters as for the smaller clusters dealt with here. The presence of extra layers of atoms, however, leads to a greater number of nodes parallel to the principal axis (*i.e.* the  $L$  quantum number is higher). For some of the larger clusters it is also necessary to consider the interaction of three or more subsets of atoms (trispherical, tetraspherical *etc.*). Such clusters will be dealt with more thoroughly in a subsequent paper.<sup>21</sup>

### Acknowledgements

The S.E.R.C. is thanked for financial support.

### References

- 1 K. Wade, *Adv. Inorg. Chem. Radiochem.*, 1976, **18**, 1; D. M. P. Mingos, *Nature (London), Phys. Sci.*, 1972, **236**, 99.
- 2 A. J. Stone, *Mol. Phys.*, 1980, **41**, 1339; *Inorg. Chem.*, 1981, **20**, 563; A. J. Stone and M. J. Alderton, *ibid.*, 1982, **21**, 2297; A. J. Stone, *Polyhedron*, 1984, **3**, 1299.
- 3 P. Brint, J. P. Cronin, and E. Seward, *J. Chem. Soc., Dalton Trans.*, 1983, 675.
- 4 P. W. Fowler, *Polyhedron*, 1985, **4**, 2051; P. W. Fowler and W. W. Porterfield, *Inorg. Chem.*, 1985, **24**, 3511.
- 5 K. Wade and M. E. O'Neill, *Inorg. Chem.*, 1982, **21**, 461.
- 6 A. Ceulemans, *Mol. Phys.*, 1985, **54**, 161.
- 7 D. B. Redmond, C. M. Quinn, and J. G. R. McKiernan, *J. Chem. Soc., Faraday Trans.*, 2, 1983, 1791.
- 8 R. L. Johnston and D. M. P. Mingos, *Polyhedron*, in the press.
- 9 (a) J. Bould, N. N. Greenwood, J. D. Kennedy, and W. S. McDonald, *J. Chem. Soc., Chem. Commun.*, 1982, 465; (b) J. Bould, J. E. Crook, N. N. Greenwood, J. D. Kennedy, and W. S. McDonald, *ibid.*, p. 346; (c) J. E. Crook, M. Elrington, N. N. Greenwood, J. D. Kennedy, and J. D. Woollins, *Polyhedron*, 1984, **3**, 901; (d) J. E. Crook, M. Elrington, N. N. Greenwood, J. D. Kennedy, M. Thornton-Pett, and J. D. Woollins, *J. Chem. Soc., Dalton Trans.*, 1985, 2407; (e) H. Fowkes, N. N. Greenwood, J. D. Kennedy, and M. Thornton-Pett, *ibid.*, 1986, 517; (f) J. D. Kennedy, *Inorg. Chem.*, 1986, **25**, 1986.
- 10 R. T. Baker, *Inorg. Chem.*, 1986, **25**, 109.
- 11 R. L. Johnston and D. M. P. Mingos, *Inorg. Chem.*, 1986, **25**, 3321.
- 12 R. L. Johnston and D. M. P. Mingos, 1986, 918.
- 13 M. J. Attfield, J. A. K. Howard, A. N. deM. Jelfs, C. M. Nunn, and F. G. A. Stone, *J. Chem. Soc., Chem. Commun.*, 1986, 918.
- 14 A. W. Duff, K. Jonas, R. Goddard, H.-J. Kraus, and C. Kruger, *J. Am. Chem. Soc.*, 1983, **105**, 5479.
- 15 R. L. Johnston and D. M. P. Mingos, *J. Organomet. Chem.*, 1985, **280**, 407.
- 16 K. Wade and M. E. O'Neill, *Polyhedron*, 1983, **2**, 963.
- 17 D. N. Cox, D. M. P. Mingos, and R. Hoffmann, *J. Chem. Soc., Dalton Trans.*, 1981, 1788.
- 18 R. L. Johnston and D. M. P. Mingos, unpublished work.
- 19 P. R. LeBreton, S. Urano, M. Shahbaz, S. L. Emery, and J. A. Morrison, *J. Am. Chem. Soc.*, 1986, **108**, 3937.
- 20 L. D. Brown and W. N. Lipscomb, *Inorg. Chem.*, 1977, **16**, 2989; J. Bicerano, D. S. Marynick, and W. N. Lipscomb, *ibid.*, 1978, **17**, 2041, 3443.
- 21 R. L. Johnston and D. M. P. Mingos, *J. Chem. Soc., Dalton Trans.*, in the press.